Anisotropy Effects in Methyl Chloride Ionization by Metastable Neon Atoms at Thermal Energies

M. Albertí* and J. M. Lucas

Departament de Química Física i Centre Especial de Recerca en Química Teòrica, Universitat de Barcelona, Barcelona, Spain

B. Brunetti,* F. Pirani, and M. Stramaccia

Dipartimento di Chimica, Università di Perugia, 06123 Perugia, Italy

M. Rosi and F. Vecchiocattivi*

Istituto per le Tecnologie Chimiche, Università di Perugia, 06124 Perugia, Italy

Received: September 22, 1999; In Final Form: December 14, 1999

Quasiclassical trajectory calculations have been carried out for the Penning ionization reaction $Ne^*(^3P_{2,0}) + CH_3Cl \rightarrow CH_3Cl^+(X, A, B) + Ne + e^-$. The calculations have been performed, within the rigid rotor approximation, for the translational energy range of 0.04−0.2 eV. The interaction potential of the colliding Ne^*-CH_3Cl system has been semiempirically estimated. The ionization probability has been determined, within the assumption that ionization occurs at the turning point, using a model which takes into account both geometry of the intermediate complex and ab initio electron density distribution of the orbitals involved on ionization. Calculations carried out for different rotational states ($j = 0$, 7, 14, 21, and 28, being $j = 14$ the most populated rotational level at 300 K) manifest the influence of CH_3Cl rotation on partial (that is for specific X, A, B electronic states of CH_3Cl^+) and total ionization. Results averaged for the populated rotational levels at 300 K show that total ionization cross section decreases with translational energy. The branching ratio to X and A states also decreases, while that to the B state increases. These results fairly reproduce previous experimental results on the energy dependence total ionization cross section and branching ratios for the production of CH_3Cl^+, CH_2Cl^+, and CH_3^+ ions.

A. Introduction

The collision of an electronically excited atom A* with a target molecule BC, characterized by an ionization potential lower than the atom excitation energy, can lead to autoionization of the intermediate complex, $A^* + BC \rightarrow [A\cdots BC^+] + e^-$. The $[A\cdots BC^+]$ complex then continues the collision leading to the formation of final product ions. In addition to BC^+ ions in different vibronic states (Penning ionization), stable associate ions ABC^+ can be formed (associative ionization). Moreover, other ions can be produced such as AB^+, the product of a postionization ion−molecule reaction between ground state A and BC^+ (rearrangement ionization), or B^+ or C^+, as result of fragmentation of excited primary BC^+ ions (dissociative ionization).[1,2]

In general, interaction anisotropy effects are expected to be very significant in these collisional autoionization processes. This can be easily understood when the commonly accepted electron exchange mechanism, originally proposed by Hotop and Niehaus[3], is taken into account. According to this mechanism, autoionization occurs through a transfer of an outer-shell electron of the target, BC, into the inner-shell vacancy of the excited atom, A*, which subsequently ejects the external electron. The obvious requirement for this process is the overlap of the orbitals involved in the electron transfer. Therefore, probability of ionization is expected to be maximum at the turning point and for approaches of the metastable atom along the directions of maximum electron density of the orbital to be ionized. This implies that probability of ionization depends on the geometry of the collisional complex at the turning point.

This aspect has recently stimulated several experimental and theoretical studies on atom−molecule systems. Ohno and coworkers[4−12] have recently measured the kinetic energy dependence of the partial ionization cross sections, i.e., for the production of specific electronic states of the primary ion, in collisions of $He^*(^3S)$ atoms with several simple molecules. They found that the partial cross sections show different energy dependences according to a combination of the anisotropy of the metastable atom−target interaction and the anisotropy of the electron density distribution of the orbitals involved in the process. For example, in the prototypical system $He^*(^3S)-N_2$ it has been found that the approach of the metastable atom toward the "side" or the "end" of the molecule leads to different population ratio of $N_2^+(X^2\Sigma)$, $N_2^+(A^2\Pi)$, or $N_2^+(B^2\Sigma)$. Moreover, specific regions of the interaction, where the electron density of the orbital to be ionized is high, produce a specific energy dependence of each partial ionization cross section.[7,12] These anisotropy effects have been recently confirmed by the measurement of the two-dimensional collision-energy/electron-energy spectrum for $He^*(^3S)-N_2$, which allowed the characterization of peak shifts and bandwidths in the 0.07−0.38 eV collision energy range.[11] These results have been also interpreted by classical trajectory calculation.[12] Dunlavy and Siska[13] have measured the high-resolution electron spectra in $He^*(^1S)-N_2$

10.1021/jp993401d CCC: $19.00
Published on Web 01/28/2000

collisional autoionization, at seven different collision energies. They obtained the nascent electronic state branching fractions, vibrational populations, and spectral line shifts and widths, as a function of collision energy. The analysis of these data confirmed the concerted role of anisotropy of interaction and anisotropy of orbital electron density distributions to produce the energy dependence of the observed electron spectra characteristics. In that work, the authors clearly get into focus how electron spectroscopy in Penning ionization represents a form of transition state spectroscopy of the process. Recently, Brunetti et al.[14] measured the energy dependence of the fragmentation pattern in the ionization of methyl halides by collision with metastable neon atoms. In that case, experimental observations were also attributed to anisotropy effects.

From a theoretical point of view, collisional autoionization phenomena are generally treated on the basis of a local complex potential whose real part represents the interaction between the colliding particles and the imaginary part (energy width) is related to the ionization probability of the system.[1,2] For the simplest case of an atom−diatom system, both real and imaginary parts are expected to be anisotropic. Therefore, the system should be described by a local complex potential energy surface (PES) depending on three coordinates,

$$W(R,r,\theta) = V_0(R, r, \theta) - (i/2)\Gamma(R,r,\theta)$$

where R is the distance from the atom to the center-of mass of the molecule, r is the internuclear distance of the diatom, and θ is the angle formed by **R** and **r** vectors. Owing to the parametric dependence of PES on internuclear distances, the determination of such complex surfaces represents a formidable problem for most polyatomic systems. Thus, for large systems, some simplifications are often introduced to reduce the dimensionality of the problem.

Being the calculation of complex interactions a difficult problem, theoretical studies on anisotropy effects in Penning ionization are very scarce, to date. Only few cases of rigorous atom−molecule treatments are present in the literature, such as the cases of $He^*(2^3S) + H_2$,[15] N_2,[12,16,17] and H_2O.[18,19] In these cases, ab initio complex potentials have been calculated and the ionization dynamics has been investigated by using quantum models or quasiclassical trajectory methods. In many other cases, semiempirical potentials and estimated energy widths have been used to analyze experimental data.[13,14]

The motivation of this study originates from the recent work of Brunetti et al.[14] where the energy dependence of the fragmentation pattern in the ionization of methyl chloride and methyl bromide by metastable neon atoms was measured. In that work it was found that the ionization cross sections for the production of CH_3X^+, CH_3^+, and CH_2X^+ (X = Cl, Br) show different decreasing trends as a function of collision energy. The measured branching ratio indicated a relative higher production of fragment ions at higher energies. These results were qualitatively interpreted in terms of a relative increase of population of the highest electronically excited B state of CH_3X. In fact, it is known that CH_3X^+ ions originally formed in the ground electronic state (X) remain undissociated, while CH_3X^+ ions produced in the A and B excited electronic states undergo to a full fragmentation to CH_3^+ and CH_3^+ or CH_2X^+, respectively.[20,21] The origin of the relative increase of population of the B state can be attributed to a larger number of vibrorotational levels which can be reached at higher collision energies[22] or to dynamical effects which produce preferential geometries of the collision complex leading to higher B state population at increasing collision energy.[7,11−13]

A computational study on the ionization of methyl chloride by metastable neon atoms is here presented. The aim is to give a more satisfactory rationalization of the previously published experimental measurements[14] and to contribute to a deeper characterization of possible anisotropy effects by studying their influence on the energy dependence of ionization cross sections and branching ratios.

The collisional autoionization dynamics is here discussed within the frame of a classical treatment. The choice has been done on the basis of the well-known reliability of classical theory in atom−molecule collisional autoionization[12] and also on the perspective of a good physical view of the role of a preferential dynamical orientation of the atom−molecule system. A semiempirical potential energy surface has been built up. Then, ab initio electron density distribution of the orbitals involved in ionization and distribution of geometries of the collision complex at the turning point have been computed. The time spent in proximity of each turning point has been also computed for each trajectory. Finally, using a specific model, the ionization probability and cross sections have been calculated, as a function of collision energy.

In the following section, the method used for the determination of the PES is reported; in section C, the modeling and computing procedure are described; in section D, the results of calculations are discussed; and finally, in section E conclusions and perspectives are given.

B. Potential Energy Surface

The most current way to determine an analytical PES is to calculate ab initio relevant points of the interaction region and then to build up a function capable of interpolating these points, connecting them smoothly and in a physically reasonable way. For this purpose, a large number of good quality ab initio points is needed. For most of polyatomic systems, this kind of study can be untreatable and some simplifications are often introduced. In fact, several interaction potentials have been constructed by reducing some degrees of freedom, in particular, studies on Penning ionization have been carried out considering that the equilibrium geometry of the molecule is kept fixed during the collision process.[9] Furthermore, the calculation of excited states is a very complex task and therefore several studies involving metastable atoms have been made substituting the metastable by the "similar" alkali atom.[9−12] This fact suggested to us the use of semiempirical methods, quite popular in the field of chemical dynamics, mainly for processes involving medium-sized molecules, complicated electronic structures, excited electronic states, or nonadiabatic effects.[23]

In the present study, the real part of the potential was obtained semiempirically. Actually, in the case of weak interaction of the order of a few tenths of electronvolts, semiempirical estimates appear to be more reliable than standard ab initio calculations. The energy widths (imaginary part of the potential) were computed using ab initio electron density distribution of molecular orbitals involved in the ionization.

The main simplifications in the calculation were introduced to reduce the dimensionality of the problem. Thus, the CH_3Cl was considered as a hypothetical diatomic A-Cl molecule where A shows a behavior very close to the CH_3 group; this approximation has been proved to be reliable in many other dynamical studies.[24−28] Also, it was assumed that the geometry of the molecule does not change during the collision.[9] Thus, our potential depends only on two variables: R, the distance between Ne* atom and the center of C−Cl bond, and θ, the angle formed by the **R** vector and C−Cl bond. This potential

can be schematically represented as

$$W(R,\theta) = V_0(R,\theta) - (i/2)\Gamma(R,\theta)$$

The semiempirical method here used starts from the identification of the components which mainly contribute to the overall interaction. Then, a suitable parametrization of such contributions is proposed, taking into account the expected relative contribution of the various terms in each region of the PES.

The real part of the PES was built up using the correlation rules recently developed in our laboratory,[29−35] which have been proven to give reliable information when the system is characterized by pure van der Waals interaction or by a van der Waals plus a weak chemical contribution.

In our previous paper,[14] the general features of Ne*−CH_3Cl interaction have been already discussed and indications on its anisotropy have been proposed. Since the results of dynamical studies strongly depend on fine details of the intermolecular potential, a more accurate study of the characteristics of the colliding system has been here accomplished. Substantially, the contributions of three interaction components have been explicitely taken into account: (a) a van der Waals term (V_{vdW}), which results from the combination of a short-range repulsion, due to the size of outer electronic orbitals, with a long-range attraction, due to dispersive and inductive forces; (b) a weak chemical contribution (V_{CC}), which arises from a configuration interaction with a close higher-lying ion-pair state originated by an electron transfer from Ne* to CH_3Cl; (c) an electrostatic term (V_{c-pd}), which comes from the interaction between the permanent C−Cl dipole and a partial positive charge on Ne* produced by a transfer of its excited electron into a sp hybrid orbital. This latter effect appears essentially at short distances and preferentially around the directions of the two lone pair orbitals of the Cl atom.

According to the above considerations, the semiempirical analytical function which describes the interaction has a different behavior for θ angles in the 0−90° range (0° is referred to the direction of C−Cl bond with the approach of metastable neon to the Cl side) and for θ angles in the 90−180° range

$$V_0(R,\theta) = V_1(R,\theta)\,F(\theta) + [1 - F(\theta)]V_{c-pd}(R) \quad 0° < \theta < 90°$$

$$V_0(R,\theta) = V_1(R,\theta) \quad 90° < \theta < 180°$$

$V_1(R,\theta)$ consists of the sum of two terms, $V_1(R,\theta) = V_{vdW} + V_{CC}$, describing the van der Waals interaction (V_{vdW}) and the weak chemical contribution (V_{CC}). As for systems involving alkali atoms, the van der Waals interaction was represented by a Lennard-Jones (8-6) function

$$V_{vdW}(R,\theta) = \epsilon(\theta)[3(R_m(\theta)/R)^8 - 4(R_m(\theta)/R)^6]$$

where $\epsilon(\theta)$ and $R_m(\theta)$ represent the potential well depth and its position as a function of θ. Their values have been obtained using the correlation formulas developed in our laboratory for the atom−diatom case, based on spherical polarizability for the atom and parallel and perpendicular polarizabilities for the molecule.[29−35]

The term V_{CC} takes the following form

$$V_{CC}(R,\theta) = -7456\cos^2\theta\exp(-1.10R)$$

as already explained in ref 14.

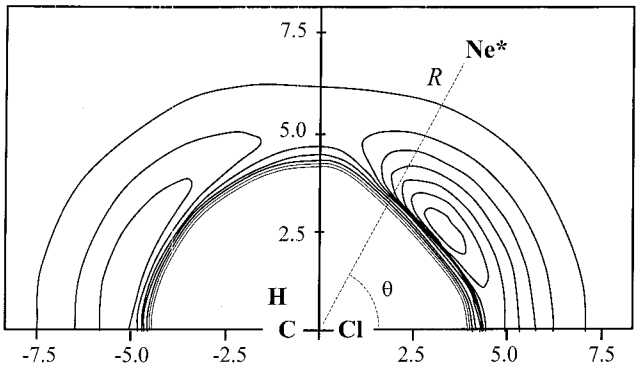

Figure 1. Contour plot for the real part of the Ne* + CH_3Cl interaction potential. The lowest curve correspond to −70 meV, and contours are spaced by 10 meV. Distances are in angstroms.

The $V_{c-pd}(R)$ term, which represents an ion−permanent dipole interaction, was described by means of a Lennard-Jones (11-2) potential function, as follows:

$$V_{c-pd}(R) = \epsilon_{c-pd}[{}^2/_9(R_{c-pd}/R)^{11} - {}^{11}/_9(R_{c-pd}/R)^2]$$

where ϵ_{c-pd} has been taken as 300 meV and R_{c-pd} as 3.5 Å. These values have been estimated through the assumption of a 0.5 effective charge on Ne* and the value of the C−Cl permanent electric dipole.

Finally, a switching function, $F(R,\theta)$, was chosen to modulate the contribution of V_1 and V_{c-pd} to V_0 in the 0−90° range, to ensure the continuity of the analytical PES and that of their derivatives, and to produce a maximum effect at the angle of 45°, that is approximately along the Cl lone pair direction within the molecule.

$$F(R,\theta) = 1/\{1 + [\exp((3.5 - R)/0.7)]\sin^2(2\theta)\}$$

The terms deriving from an ion-induced dipole interaction are here neglected because they are expected to be very weak. It is obvious that a change of the switching function can significantly modify the angular dependence and shape of the surface. However, test calculations indicated that reasonable modifications of the switching function did not substantially change the results described in section D.

A view of the potential energy surface is reported in Figure 1, where a contour plot of the anisotropic potential for a neon metastable atom approaching to a rigid CH_3Cl molecule is shown. The lowest curve corresponds to an energy of −70 meV, and the contour lines are spaced by 10 meV. The distances are given in angstroms.

Concerning with the imaginary part of the optical potential (potential energy width), here we anticipate that it has been considered equal to the sum of three different exponential functions each one corresponding to the ionization into the three X, A, and B states of the CH_3Cl^+ ion. These functions have been chosen to follow the exponential decay, on distance and angles, of electron density distributions of each one of the three orbitals (see Figure 2).The density distribution has been computed ab initio, employing a basis set of triple-ζ valence quality augmented with a polarization function. The geometry of the molecule has been optimized at the SCF level, assuming a C_{3v} symmetry, using gradient techniques.[14] The calculations were performed by the use of the GAMESS program package implemented on a cluster of RISC6000 workstations.

A more detailed explanation of the characteristics and properties of the potential energy width used in the present study is given in the following section.

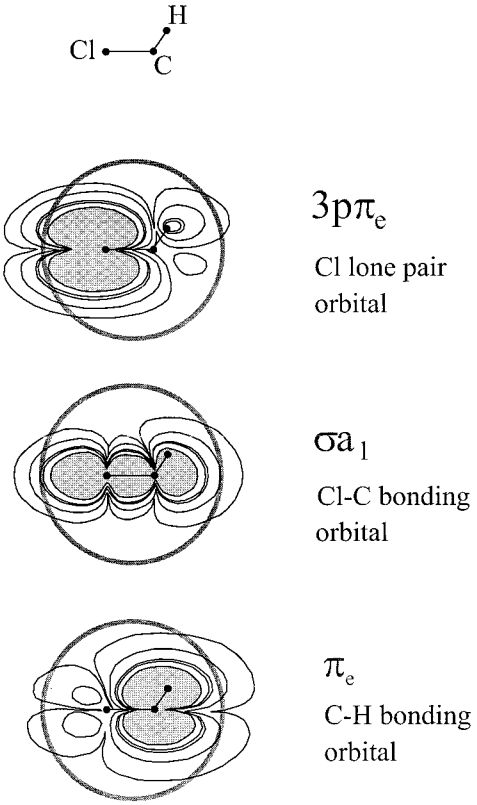

Figure 2. Electron density maps of the three outer orbitals of CH_3Cl involved in ionization with metastable neon atoms. The van der Waals average size of the molecule is also shown in order to indicate the parts of the orbitals which are more efficiently ionized.

C. Modeling and Computing Procedure

Extensive quasiclassical trajectory calculations have been carried out to compute the collision energy dependence of ionization cross sections and branching ratios for the formation of the different electronic states (X, A, and B) of CH_3Cl^+. A total of 50 000 trajectories were run for each set of initial conditions, thus ensuring a very good statistics. Seven translational energies from 0.04 to 0.2 eV were analyzed for five different rotational states of the "diatom" corresponding to j = 0, 7, 14, 21, and 28. Trajectories were initiated when the Ne* atom was at a distance of 20 Å from the center of mass of the CH_3Cl molecule, this distance being large enough to consider negligible any interaction between the colliding particles. The time step size was fixed to 5.0×10^{-16} s. The maximum impact parameter, b_{max}, was taken originally to be equal to 10 Å, then its value was corrected following a procedure described in the next section.

The starting point was to consider the ionization probability for each trajectory in a classical treatment[17]

$$P_{ion}(t) = 1 - \exp[-\int_{-\infty}^{t} W(t)\,dt] \qquad (1)$$

where

$$W(t) = \frac{\Gamma(R,\theta)}{\hbar} \qquad (2)$$

The inverse of $W(t)$ represents the lifetime of the system, τ, when the geometry of the intermediate is defined by R and θ. Here, R is the distance between the metastable atom and the center of mass of CH_3Cl and θ is the angle formed by **R** and C−Cl bond.

Taking into account that ionization mainly occurs at the turning point, eq 1 can be approximated to the following form:

$$P_{ion}(R_0,\theta_0) = 1 - \exp\left[\frac{\Gamma(R_0,\theta_0)}{\hbar}\Delta t\right] \qquad (3)$$

where Δt is the finite time spent by the system in the vicinity of the turning point, defined by the distance R_0 and angle θ_0.

The values of R_0 and θ_0 for each trajectory, and therefore the geometry of the collision complex at the instant of ionization, were determined from the analysis of the derivatives of the distance R respect to the time along the trajectory, $\dot{R}$. As R_0 and θ_0 we have taken the values of R and θ where the trajectory changes from a value of $\dot{R} < 0$ to $\dot{R} > 0$. It has been checked that the turning point so defined is unique for all the trajectories in our system. For each trajectory, the time spent by the system in the vicinity of turning point, Δt, was defined as the time spent from $R_0 + 0.1$ Å (for $\dot{R} < 0$) to $R_0 + 0.1$ Å (for $\dot{R} > 0$).

Introducing the lifetime of the system, $\tau = \hbar/\Gamma(R,\theta)$, eq 3 can be written as

$$P_{ion}(R_0,\theta_0) = 1 - \exp\left[\frac{\Delta t}{\tau(R_0,\theta_0)}\right] \qquad (4)$$

This equation clearly describes the physics of the process; the ionization probability depends on the ratio of the time spent in the vicinity of the turning point and the corresponding local lifetime. P_{ion} can be computed when $\Gamma(R,\theta)$ is known.

In the present model, we have considered the additivity of the partial widths

$$\Gamma = \Gamma_X + \Gamma_A + \Gamma_B \qquad (5)$$

To consider the potential widths as additive modifies the multiple-final-state problem into a set of single-channel independent processes, neglecting any possible coupling between them. Although the partial cross sections do not precisely add to give the total ionization cross section, as discussed by Dunlavy and Siska,[13] this problem appears to be more significant when the total cross section shows a strong energy dependence. Since in our case the energy dependence of the total ionization cross section in the investigated energy range is not very pronounced,[14] we have considered this approximation as justified.

As already mentioned in the previous section, for the computation of the ionization probability, we have assumed that, for the three states, $\Gamma_i(R,\theta)$ is proportional to the electron density distribution, $D_i(R,\theta)$, of the corresponding orbital to be ionized, according to the formula

$$\frac{\Gamma_i(R,\theta)}{\hbar} = a_i D_i(R,\theta) \qquad (6)$$

where a_i is the proportionality constant and i = X, A, or B. This is equivalent to choosing an empirical exponential function whose trend follows the decay of electron density of the various orbitals. By this method, the ionization cross sections, as a function of collision energy, can be calculated for the three separated electronic states of the primary ion.

The three constants, a_X, a_A, and a_B can be estimated to scale $\Gamma_i(R,\theta)$ in order to reproduce the branching ratios and total ionization probability (as obtained from total ionization cross section divided by πb^2_{max}) at the intermediate value of the collision energy experimentally investigated, 0.07 eV. The procedure is explained in the following.

As a consequence of the additivity of the three Γ_i, the total ionization probability described by eq 3 can be written as

$$P_{ion}(R_0,\theta_0) = 1 - \exp\left[-\frac{\Gamma_X(R_0,\theta_0)}{\hbar}\Delta t\right] \times \exp\left[-\frac{\Gamma_A(R_0,\theta_0)}{\hbar}\Delta t\right]\exp\left[-\frac{\Gamma_B(R_0,\theta_0)}{\hbar}\Delta t\right] \quad (7)$$

and therefore the partial ionization probabilities P_i, for ionization into each one of the three possible states, can be expressed by

$$P_i(R_0,\theta_0) = g_i\left\{1 - \exp\left[-\frac{\Gamma_X(R_0,\theta_0)}{\hbar}\Delta t\right] \times \exp\left[-\frac{\Gamma_A(R_0,\theta_0)}{\hbar}\Delta t\right]\exp\left[-\frac{\Gamma_B(R_0,\theta_0)}{\hbar}\Delta t\right]\right\} \quad (8)$$

where g_i corresponds to the g_X, g_A, or g_B constants. These values are the branching ratios for the ionization into the three X, A, or B states, such that

$$g_X + g_A + g_B = 1 \quad (9)$$

From eq 8 follows

$$\frac{g_X}{g_A} = \frac{P_X(R_0,\theta_0)}{P_A(R_0,\theta_0)} \quad (10)$$

with similar expressions for the g_X/g_B and g_A/g_B ratios.

If one assumes that

$$\frac{P_X(R_0,\theta_0)}{P_A(R_0,\theta_0)} = \frac{g_X}{g_A} \approx \frac{1 - \exp\left[-\frac{\Gamma_X(R_0,\theta_0)}{\hbar}\Delta t\right]}{1 - \exp\left[-\frac{\Gamma_A(R_0,\theta_0)}{\hbar}\Delta t\right]} \quad (11)$$

and similar expressions for P_X/P_B, it can be found from eqs 3 and 7 that

$$c_1 \exp\left[-\frac{\Gamma_X(R_0,\theta_0)}{\hbar}\Delta t\right] + c_2\left\{\exp\left[-\frac{\Gamma_X(R_0,\theta_0)}{\hbar}\Delta t\right]\right\}^2 + c_3\left\{\exp\left[-\frac{\Gamma_X(R_0,\theta_0)}{\hbar}\Delta t\right]\right\}^3 = \exp\left[-\frac{\Gamma(R_0,\theta_0)}{\hbar}\Delta t\right] \quad (12)$$

where the c_i constants are related to the branching ratios to the three electronic states by the following equations:

$$c_1 = 1 - \frac{g_B + g_A}{g_X} + \frac{g_A g_B}{{g_X}^2}$$

$$c_2 = \frac{g_B + g_A}{g_X} - 2\frac{g_A g_B}{{g_X}^2}$$

$$c_3 = \frac{g_A g_B}{{g_X}^2} \quad (13)$$

At a fixed collision energy (we chose 0.07 eV), in eq 12 only $\Gamma_X(R_0,\theta_0)$ is unknown and its value can be determined. The same can be done to obtain $\Gamma_A(R_0,\theta_0)$ and $\Gamma_B(R_0,\theta_0)$. Finally, by combining eqs 6, 12, and 13, the three a_X, a_A, and a_B constants can be determined. It can be noted that eq 12 has three solutions but only one is good because only one is real and positive.

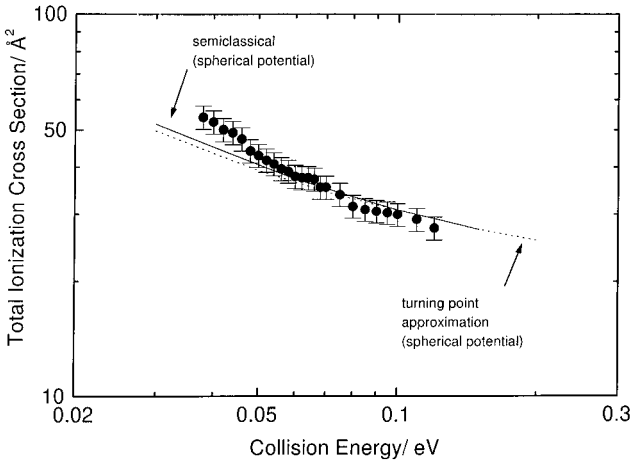

Figure 3. Total ionization cross sections for Ne*−CH_3Cl collisions as obtained using a spherically averaged optical potential. The two curves are the results of a semiclassical calculation and the classical procedure of the present work (see text). Experimental cross sections are from ref 14.

Once the proportionality constants are known, both partial and total ionization probabilities for different values of translational energy can be easily calculated. In fact, from the total ionization probability, the total cross section can be obtained by means of

$$\sigma(E) = \pi {b_{max}}^2 \overline{P_{ion}}(E) \quad (14)$$

where $\overline{P_{ion}}$ is the average over all trajectories with impact parameter lower than b_{max} at a fixed translational energy. Similar equations can be used for partial cross sections

$$\sigma_i(E) = \pi {b_{max}}^2 \overline{P_i}(E) \quad (15)$$

D. Results and Discussion

The validity of the whole modeling and calculation procedure of the present work lies primarily on the validity of the assumption that ionization only occurs at the turning point of the collision. Although this assumption has been successfully used in dynamical studies of other Penning ionization systems,[36,37] its validity has been verified for the present case. To this purpose, total ionization cross sections as a function of collisional energy have been calculated by using a Ne*−CH_3Cl spherically averaged optical potential, obtained averaging the potential energy surface of the previous section over its angular dependence. The cross sections have been computed following both a semiclassical computational procedure and the classical procedure of the turning point model discussed above. The semiclassical calculation has been performed computing the complex phase shift within the JWKB approximation. The classical calculation is the same described in the previous section with the simplification of the lack of the angular dependence of the complex potential. The results of the two calculations are compared in Figure 3. Since the classical model of the present work calculates "relative" cross sections as a function of collision energy, the classical cross sections have been normalized to the absolute value of the semiclassical cross section at the intermediate collision energy of 0.07 eV. It appears that the two sets of cross sections show an almost identical energy dependence with a maximum divergence of only 3% in the low-energy limit presently investigated. The validity limits of the turning point approximation have been further checked

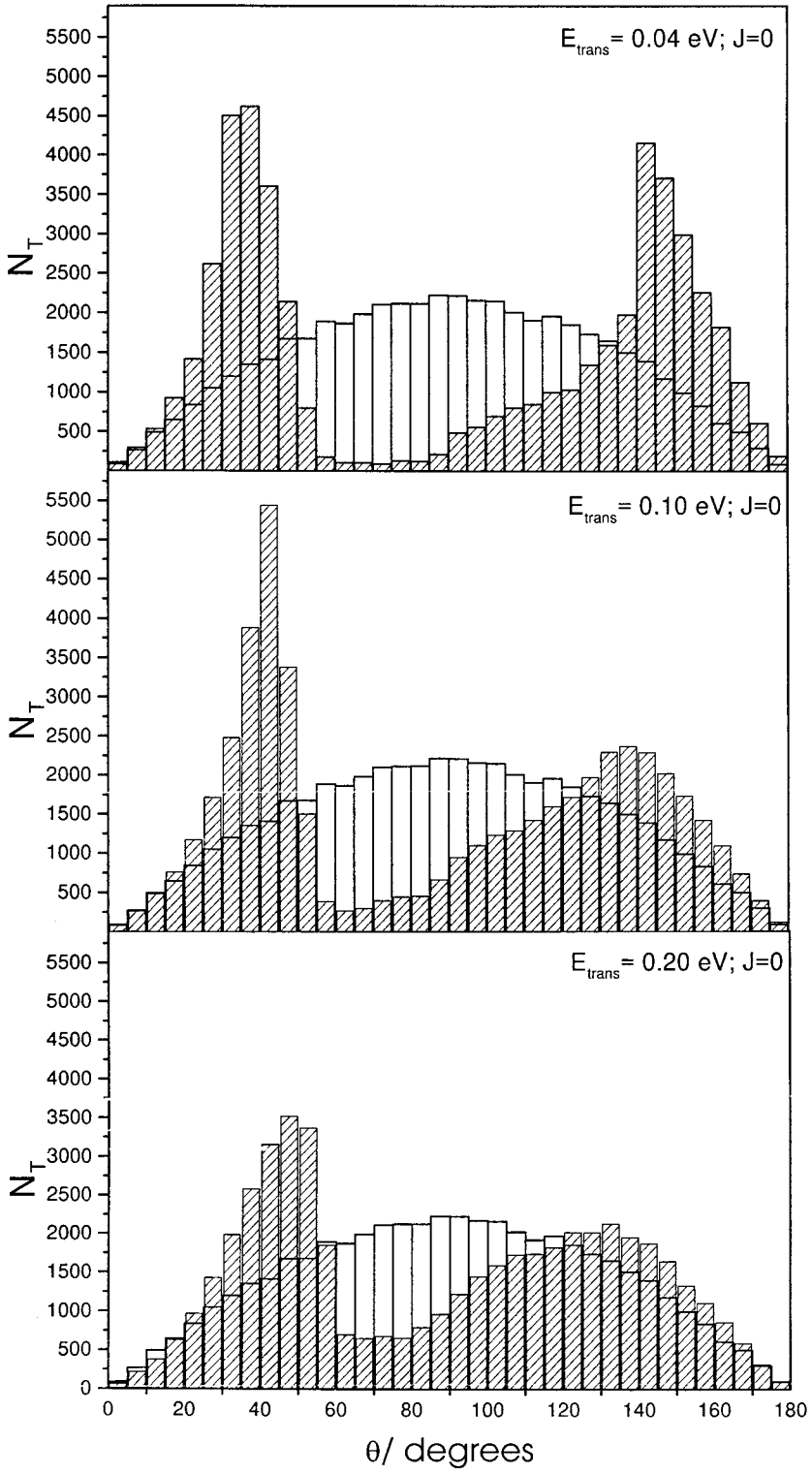

Figure 4. Distribution of geometries of the collision complex at the turning point (number of trajectories for each θ angle) at three different collision energies, for $J = 0$. The starting point cosine law distribution is also shown for comparison.

by performing analogous calculations for specific "cuts" of the PES. In all the cases the deviation between semiclassical calculations and turning point approximation was always less than 5%. These results can be considered as a good indication that the assumption of autoionization at the turning point is valid in the present case and that the classical model here adopted is satisfactory for the calculation of the energy dependence of ionization cross sections.

An advantage of the present classical model is the possibility to analyze possible reorientation effects of the particles due to their interaction during the collision. In fact, it is possible to put in evidence how the collision dynamics can produce specific preferential geometries of the collisional complex at the turning point, that is, specific geometries at the instant of the ionization event. In Figures 4 and 5 are reported the distribution of orientation angles, θ, at the turning point for the neon metastable atoms approaching to the center of mass of CH_3Cl, for all the computed trajectories. In every plot, the original distribution of the statistical starting points is shown for comparison, as a white histogram. In Figure 4, it is clearly shown how reorienta-

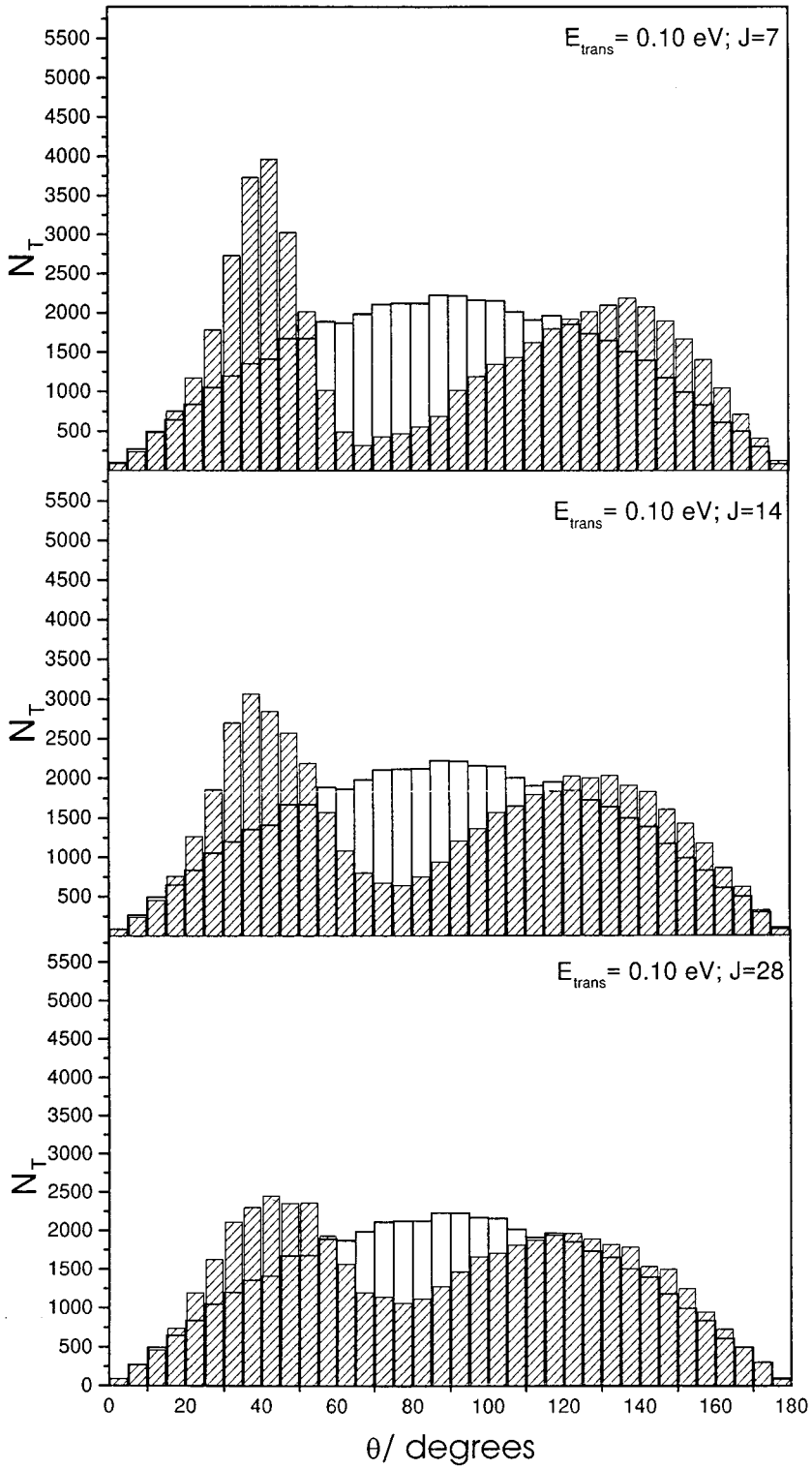

Figure 5. Distribution of geometries of the collision complex at the turning point (number of trajectories for each θ angle) at a collision energy of 0.1 eV, for $J = 7$, 14, and 28. The starting point cosine law distribution is also shown for comparison.

tion effects are largely present for all the collision energies for the lowest rotational state, $j = 0$, of CH_3Cl. In Figure 5, it is shown how these effects are significantly present also for the higher rotational levels and higher collision energies.

The plots reported in Figures 4 and 5 clearly show that, for the present collision energies, rotational temperature, and interaction potential, the collision dynamics produces turning point complexes characterized by preferential geometries with θ_0 angles of around 40° and 130°. This effect tends to be smoothed out going toward higher energies.

The analysis of the turning point calculation at different collision energies allows us to perform some additional considerations. In Figure 6 the turning point distance, R_0, as a function of the impact parameter, b, are reported for a typical collision energy, chosen as 0.07 eV. The points of the figure correspond to all θ angles, that is, to any possible geometry of the collision complex without any distinction. The dependence of R_0 on b shows a pronounced change at a certain value of b, indicated as b_{lim}. For b from 0 to b_{lim}, the R_0 values increase slowly with impact parameter. For b values larger than b_{lim},

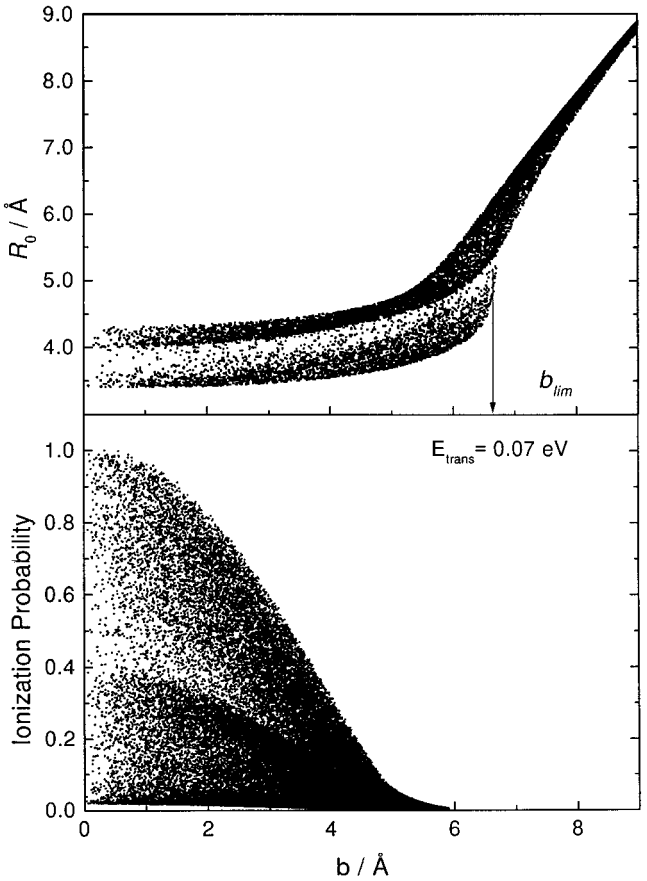

Figure 6. Dependence of R_0 versus impact parameter (upper panel) and total ionization probability versus impact parameter (lower panel) at a collision energy of 0.07 eV.

the increase becomes sharp, with a slope close to unity. This slope implies that R_0 has approximately the same value of the impact parameter, b. This is expected for straight trajectories, that is, when no interaction is present between the metastable atom and the target. In Figure 6, the probability of total ionization, as obtained in the present calculation, is also reported as a function of the impact parameter, for the same collision energy. It can be noted that the value of b_{lim} is close to the value of b_{max} for total ionization. This correspondence has been found to be present not only at 0.07 eV but at all the collision energies of the present calculations. This observation implies the following considerations: (a) within the present model, b_{lim} can be used in place of b_{max}, being b_{lim} large enough to ensure that trajectories with larger impact parameters have an ionization probability equal to zero for all the three electronic states; (b) since collisional autoionization occurs only for impact parameters lower than b_{lim} and substantial reorientation of the colliding system occurs, it can be concluded that ionization occurs for trajectories mainly determined by long-range attractive forces. The latter consideration fits well with the observed decreasing energy dependence of total ionization cross section.[6−13,38]

Different geometries of the collision complex at the turning point are expected to be related to different populations of the three electronic states of the methyl chloride ion according to the different electron density distribution of the orbitals involved in ionization (see Figure 2). In Figures 4 and 5, it has been clearly shown how collision energy and rotational state of CH_3Cl influence the formation of autoionizing complexes with specific geometries. It is therefore obvious that the influence of CH_3Cl rotation must be properly taken into account in the calculation of ionization cross section as a function of collisional energy.

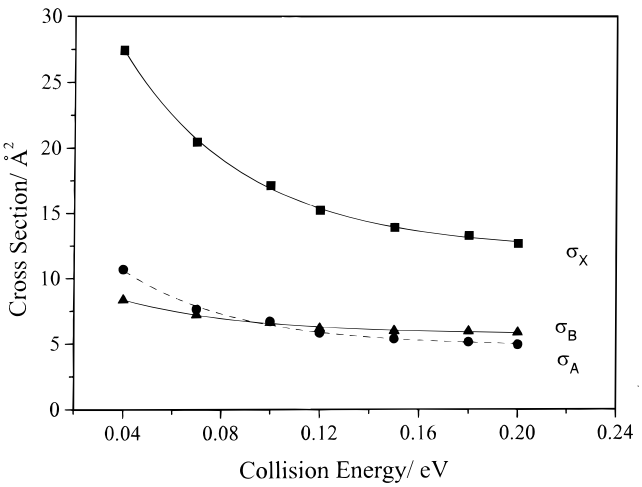

Figure 7. Partial ionization cross sections for the formation of the three X, A, and B electronic states of CH_3Cl^+, as a function of collision energy. The computed cross sections have been scaled to reproduce the absolute value of total cross sections and a population ratio 100/40/30 at 0.04 eV (see text).

The range of j values populated at 300 K (from $j = 0$ up to $j = 50$) is too large to make trajectory calculations for all of them. Thus, the contribution of the rotation for the formation of each one of the three electronic states of CH_3Cl^+ was included in an averaged form. As a first step, a study of the influence of the rotation on partial and total ionization have been performed for five CH_3Cl rotational levels, $j = 0$, 7, 14, 21, and 28, being $j = 14$ the most populated rotational level at 300 K. Second, for seven different values of relative translational energy, it was observed that ionization on individual states varies linearly with j, with a slope that decreases smoothly by increasing translational energy. Finally, the above-mentioned dependence of partial ionization on j has been taken into account, together with the population of every rotational state at 300 K, and the ionization cross sections have been calculated. The results for the rotationally averaged cross sections, so obtained, are shown in Figure 7.

The partial cross sections of Figure 7 have been normalized to give a relative population ratio of the three X, A, and B states of 100:40:30, at the collision energy of 0.04 eV. These values are arbitrary, but have been chosen on the basis of the following arguments. To our knowledge, the only measurement in the literature able to give information on the relative state population of CH_3Cl^+ ions, in Ne*−CH_3Cl collisional autoionization, is the low-resolution electron energy spectrum of Čermák.[39] However, from that spectrum it is difficult to assess precisely the relative population of the three electronic states of CH_3Cl^+. In fact, while X state is clearly well separated, A and B states show two partially overlapped bands which fall in the low-energy limit of the spectrum, where a strong background is present. Similar difficulties in determining the relative populations of X, A, and B states are present in the analogous low-resolution He*−CH_3Cl electron energy spectrum of Brion and co-workers.[40] Despite these difficulties, these authors can clearly establish that in He* Penning ionization of methyl chloride the relative population of higher states (X/A/B = 100:40:40) is lower than in HeI photoionization (100:40:60). In the absence of other information, we have decided to normalize our partial cross sections to the population ratio X/A/B as 100:40:30, giving to the B state an even lower value than in He* Penning ionization, due to the lower excitation energy of neon metastable atoms compared to helium. However, it must be noted that

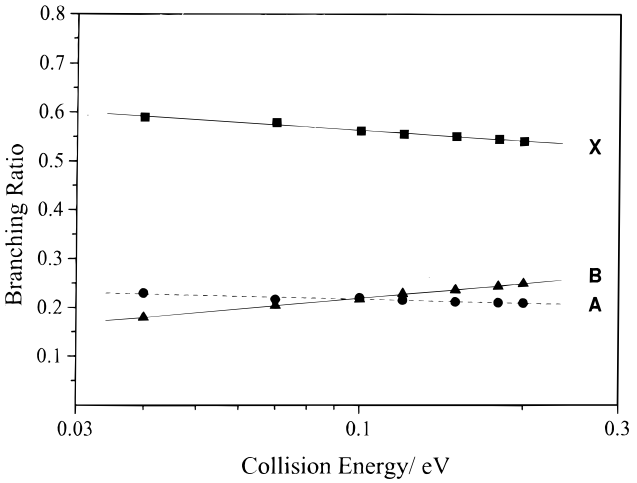

Figure 8. Branching ratio for X, A, and B state population, as a function of collision energy.

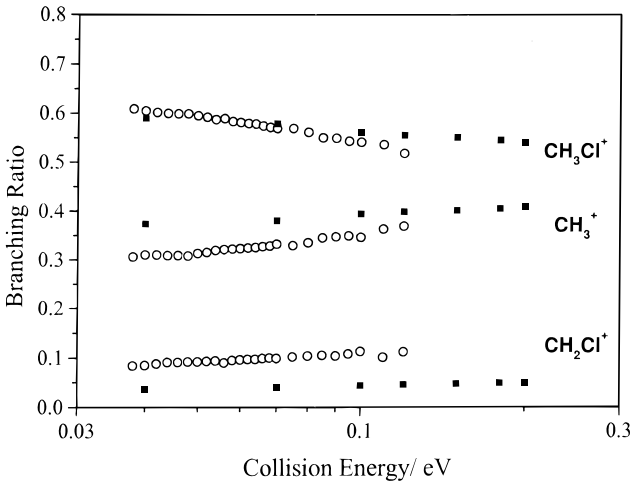

Figure 9. Theoretical and experimental branching ratio for the formation of final CH_3Cl^+, CH_3^+, and CH_2Cl^+ ions, as a function of collision energy. The branching to final products have been computed assuming that primary CH_3Cl^+(X, A, B) ions undergo fragmentation as reported in ref 21 (see text).

reasonable modifications of the X/A/B ratio do not significantly affect the final results of the present study.

The crucial point of the present results is the energy dependence of the three partial cross sections for the formation of the three ionic states, as reported in Figure 7. In fact, it is known that the collision energy dependence of Penning ionization cross sections is correlated with the attractive or repulsive nature of the interaction potential between the colliding particles.[6−13,38] In particular, it is well established that weak van der Waals and rapidly repulsive interactions generally originate increasing cross sections at increasing energy, while attractive interaction originate decreasing cross sections. In view of these considerations, ionization on X states, produced by the removal of one electron from the $3p\pi_{eX}$ orbital, largely localized on the Cl atom, reflects the probing of the most attractive PES region and partial cross sections reported in Figure 7 show a strong decrease with translational energy. The partial cross section for the B state, produced when one electron is lost by the π_e orbital, largely localized on the methyl group, shows again a decreasing trend, but less pronounced than in the previous case. The formation of the A state, due to the removal of one electron from the σa_1, which is a carbon−halogen bonding orbital, gives a cross section that reflects the characteristics of the PES near Cl atom and near CH_3 group. In fact, the partial cross section for the A state decreases with translational energy less than cross section for X state but more than cross section for B.

These relative energy dependences are reflected in the branching ratios of Figure 8 which show that the relative population of the X and A states decrease with collision energy, while that of the B state increases.

To compare partial ionization cross sections, which refer to X, A, and B states, with experimental ionic branching ratios, which refer to CH_3Cl^+, CH_2Cl^+, and CH_3^+, it is necessary to establish a relationship between the populated states and each specific product ion. Eland et al.,[21] in a photoelectron−photoion coincidence study on the dynamics of methyl halide ion dissociations, have found that when CH_3Cl^+ ions are formed in the ground state they remain substantially undissociated, while the same ions excited to the A and B state fully dissociate to fragments. In particular, CH_3Cl^+(A) leads completely to CH_3^+, while CH_3Cl^+ (B) gives rise partially to CH_3^+, through an internal conversion from B to A and partially to CH_2Cl^+ by specific dissociation from B. It has been estimated that approximately 80% of CH_3Cl^+(B) leads to internal conversion to A state.[21] Assuming that also in this case the B to A internal conversion is about 80%, the ionic branching ratio of Figure 9 have been obtained as a function of collision energy. It can be noted that the theoretical results show energy dependences that are in good agreement with the experimental ones. While the fraction of CH_3^+ and CH_2Cl^+ increases with collision energy, the fraction of CH_3Cl^+ decreases. Although the fragmentation pattern does not perfectly reproduce the experimental one, the energy dependence of the ionic branching ratio is semiquantitatively reproduced.

It is better to remark again that the classical theoretical model of the present study allows us to calculate the energy dependence of the ionization cross sections for each one of the three accessible electronic states of CH_3Cl^+. Then, the three cross sections can be scaled down to obtain the ionic branching ratio on the basis of the expected X/A/B population ratio and B to A internal conversion. It must be noted that different scaling of the three partial cross sections does not change the basic result of our calculation; anisotropy effects influence the ionization leading to a relative increase of fragment ions when collision energy increases. In fact, trial calculations allowed us to conclude that different values of the X/A/B population ratio, accompanied by B to A conversion between 60% and 80%, originate fragmentation patterns that are never too far from those of ref 14, with an energy dependence of the ionic branching ratio which always shows a relative increase of formation of CH_3^+ (and CH_2Cl^+) compared to CH_3Cl^+ at increasing collision energy, as experimentally observed. As an example, in Figure 10 it is shown that the energy dependence of the ionic branching ratio, as obtained assuming an X/A/B population ratio of 100: 40:40 and an internal B to A conversion of 60%. This case represents a fit of the experimental results.

From total ionization probability and maximum impact parameter, total ionization cross section as a function of translational energy have been calculated. In Figure 11, the experimental and theoretical total cross sections are compared. The agreement between experiment and theory is very good at medium and high translational energies, and at lower energies the theoretical value is only slightly lower, approximately 10%, than the experimental measurement. Taking into account the experimental uncertainty and the approximate nature of the model used, the agreement for the whole collision energy range

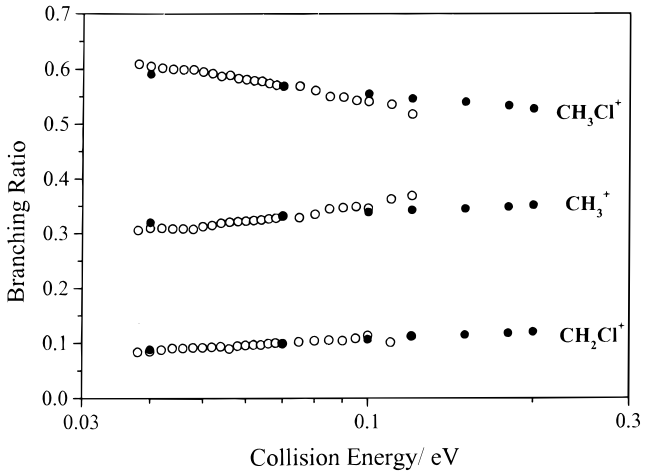

Figure 10. Branching ratio for the formation of final CH_3Cl^+, CH_3^+, and CH_2Cl^+ ions, as a function of collision energy. The branching to final products have been computed modifying the X/A/B ratio and B to A internal conversion in order to better reproduce the experimental data of ref 14 (see text).

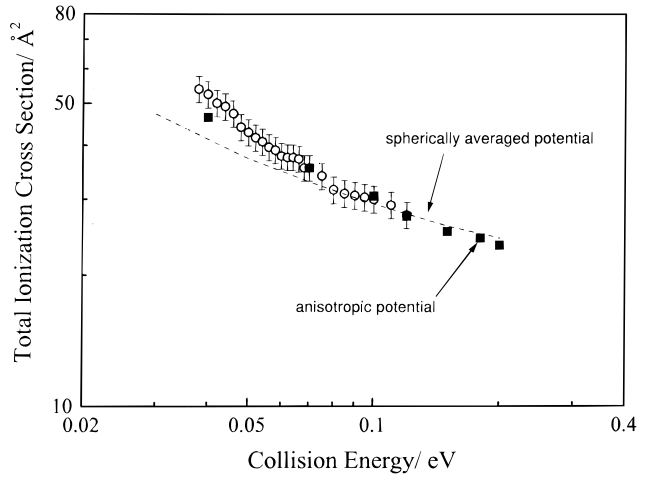

Figure 11. Total ionization cross sections, as computed in the present work (squares), with the corresponding experimental cross sections of ref 14 (circles), as a function of collision energy. For comparison, total ionization cross sections, calculated with a spherically averaged optical potential, are also reported as a dashed line.

can be considered very good. In Figure 11, the cross sections as computed assuming a spherically averaged potential are also reported as a dashed line. It can be noted how the introduction of the interaction anisotropy, leading to specific geometries of the collision complex, produces a better agreement between theoretical and experimental cross sections. This can be considered an additional indication that effectively anisotropy effects play an important role in the ionization dynamics of this system.

E. Summary and Conclusions

Quasiclassical trajectory calculations have been carried out for the ionization of methyl chloride by collision with metastable neon atoms. The calculations have been performed, within the rigid rotor approximation, for the translational energy range 0.04−0.2 eV for a CH_3Cl rotational temperature of 300 K. The interaction potential energy surface of the colliding system has been semiempirically estimated and the ionization probability has been determined, within the assumption that ionization occurs at the turning point. A specific model which takes into account the geometry of the autoionizing collisional complex and ab initio electron density distributions of the orbitals involved on ionization has been used. The results show that the total ionization cross section decreases with translational energy. The branching ratio to specific X and A electronic states of CH_3Cl^+ ions, primarily produced, also decreases as a function of collision energy, while that to B state increases. These results fairly reproduce previous experimental results on the energy dependence total ionization cross section and branching ratios for the production of CH_3Cl^+, CH_2Cl^+, and CH_3^+, as originated by possible dissociation of the three electronic states of primary CH_3Cl^+ ions. These results appear to be well correlated to the anisotropy of interaction of neon metastable atoms with methyl chloride and to the anisotropy of electron density distribution of the orbitals involved in ionization, indicating that anisotropy effects can indeed play a very important role in the collisional autoionization dynamics of this system, leading to a variation of the final ion pattern as a function of collision energy.

More details on Ne*−CH_3Cl ionization dynamics will be clarified when high-resolution electron energy spectra and, possibly, their energy dependence will be measured. Other important information is expected from Penning ionization experiments with oriented CH_3Cl molecules.[41]

Acknowledgment. M.A. and J.M.L. acknowledge partial financial support from Spanish DGCYT (Grants PB95-0598-C02-01 and PB97-0919) and the Generalitat de Catalunya (CUR Grants 1996SGR-00040 and 1998SGR-00008). M.A. is also grateful for a Visiting Professorship to the Chemistry Department of the University of Perugia from the Comissionat per a Universitats i Recerca (Generalitat de Catalunya). Financial support from italian MURST and CNR is gratefully acknowledged.

References and Notes

(1) Siska, P. E. *Rev. Mod. Phys*. **1993**, *65*, 337 and references therein.
(2) Brunetti, B.; Vecchiocattivi, F. In *Ion Clusters*; Ng, C., Baer, T., Powis, I., Eds.; Wiley & Sons, Ltd.: New York, 1993; pp 359−445 and references therein.
(3) Hotop, H.; Niehaus, A. *Z. Phys*. **1969**, *228*, 68.
(4) Ohno, K.; Harada, Y. In *Theoretical Models of Chemical Bonding*; Maksic, Z. B., Ed.; Springer-Verlag: Berlin, 1991; Part 3, pp 199−233.
(5) Ohno, K.; Mutoh, H.; Harada, Y. *J. Am. Chem. Soc*. **1983**, *105*, 4555.
(6) Mitsuke, K.; Takami, T.; Ohno, K. *J. Chem. Phys*. **1989**, *91*, 1618.
(7) Ohno, K.; Takami, T.; Mitsuke, K.; Ishida, T. *J. Chem. Phys*. **1991**, *92*, 2675.
(8) Takami, T.; Mitsuke, K.; Ohno, K. J. *Chem. Phys*. **1991**, *95*, 918.
(9) Pasinszki, T.; Yamakado, H.; Ohno, K. *J. Phys. Chem*. **1995**, *99*. 14678.
(10) Yamakado, H.; Yamauchi, M.; Hoshino, S.; Ohno, K. *J. Phys. Chem*. **1995**, *99*, 17094.
(11) Kishimoto, N.; Furuhashi, M.; Ohno, K. *J. Electron Spectrosc. Relat. Phenom*. **1998**, *88*−*91*, 143.
(12) Ogawa, T.; Ohno, K. *J. Chem. Phys*. **1999**, *110*, 3733.
(13) Dunlavy, D. C.; Siska, P. E. J. *Phys. Chem*. **1996**, *100*, 21.
(14) Brunetti, B.; Candori, P.; De Andrés, J.; Pirani, F.; Rosi, M.; Falcinelli, S.; Vecchiocattivi, F. *J. Phys. Chem. A* **1997**, *101*, 7505.
(15) Vojtik, J.; Kotal, R. *J. Phys. Chem*. **1995**, *99*, 15473. Vojtik, J.; Kotal, R. *Chem. Phys. Lett*. **1996**, *255*, 251.
(16) Ishida, T. *Chem. Phys. Lett*. **1992**, *191*, 1.
(17) Ishida, T.; Horime, K. *J. Chem. Phys*. **1996**, *105*, 5380.
(18) Ishida, T. *J. Chem. Phys*. **1995**, *102*, 4169.
(19) Ishida, T. *J. Chem. Phys*. **1996**, *105*, 1392.
(20) Lane, I. C.; Powis, I. *J. Phys. Chem*. **1993**, *22*, 5803.
(21) Eland, J. H. D.; Frey, R.; Kuestler, A.; Schulte, H.; Brehm, B. *Int. J. Mass. Spectrosc. Ion Phys*. **1976**, *22*, 155.
(22) BenArfa, M.; Lescop, B.; Cherid, M.; Brunetti, B.; Candori, P.; Malfatti, D.; Falcinelli, S.; Vecchiocattivi, F. *Chem. Phys. Lett*. **1999**, *308*, 71.
(23) Kuntz, P. J. In *Theory of Chemical Reaction Dynamics*; Michael Baer, Ed; CRC Press, Inc.: Boca Raton, FL.

(24) Solé, A. Ph.D. Thesis, Departament de Química Física, Universitat de Barcelona.
(25) Blais, N. C.; Bunker, D. L. *J. Chem. Phys*. **1963**, *39*, 315.
(26) Karplus, M.; Goodfrey, M. *J. Am. Chem. Soc*. **1966**, *88*, 5332.
(27) LaBudde, R. A.; Kuntz, P. J.; Bernstein, R. B.; Levine, R. D. *Chem. Phys. Lett*. **1973**, *19*, 7.
(28) LaBudde, R. A.; Kuntz, P. J.; Bernstein, R. B.; Levine, R. D. *J. Chem. Phys*. **1973**, *59*, 6286.
(29) Cambi, R.; Cappelletti, D.; Liuti. G.; Pirani, F. *J. Chem. Phys*. **1991**, *95*, 1852.
(30) Liuti, G.; Pirani, F. *Chem. Phys. Lett*. **1985**, *122*, 2154.
(31) Cappelletti, D.; Liuti, G.; Pirani, F. *Chem. Phys. Lett*. **1991**, *183*, 297.
(32) Aquilanti, V.; Cappelletti, D.; Pirani, F. *Chem. Phys*. **1996**, *209*, 299.
(33) Pirani, F. *Discuss. Faraday. Soc*. **1994**, *97*, 327.
(34) Pirani, F.; Cappelletti, D.; Aquilanti, V. In *Molecular Physics and Hypersonic Flows*; Capitelli, M., Ed.; Kluwer: Dordrecht, 1996.
(35) Aquilanti, V.; Cappelletti, D.; Pirani, F. *J. Chem. Phys*. **1997**, *106*, 5043. Aquilanti, V.; Cappelletti, D.; Pirani, F. *Chem. Phys. Lett*. **1997**, *271*, 216.
(36) Martin, D. W.; Weiser, C.; Sperlein, R. F.; Bernfeld, D.; Siska, P. E. *J. Chem. Phys*. **1989**, *90*, 1564.
(37) Brunetti, B.; Cambi, R.; Falcinelli, S.; Farrar, J. M.; Vecchiocattivi, F. *J. Phys. Chem*. **1993**, *97*, 11877.
(38) Aguilar, A.; Brunetti, B.; Gonzalez, M.; Vecchiocattivi, F. *Chem. Phys*. **1990**, *145*, 211.
(39) Čermák, V. *Z. Collect. Czech. Chem. Commun*. **1968**, *33*, 2739.
(40) Brion, C. E.; Stewart, W. B.; Yee, D. S. C.; Crowley, P. *J. Electron. Spectrosc. Relat. Phenom*. **1981**, *23*, 45.
(41) Ohoyama, H.; Yamato, M.; Kawaguchi, H.; Kasai, T.; Brunetti, B.; Vecchiocattivi, F. *Chem. Phys. Lett*. **1999**, *313*, 484.